

Analysis of fracture roughness parameters of S355J2 steel and EN AW-2017A-T4 aluminium alloy

Wojciech Macek^{1,*}, and Tomasz Wołczański¹

¹Opole University of Technology, Faculty of Production Engineering and Logistics, Sosnkowskiego 31, 45-272 Opole, Poland

Abstract. This article presents an analysis of fracture surface for steel S355J2 and EN AW-2017A-T4 aluminium subjected to fatigue bending, torsion, and bending with torsion. Fracture surfaces were observed using the focus variation microscope, which allows for the acquisition of data sets with large depth of focus. The authors focus on presenting the features of profile roughness parameters on the example of differences between fracture propagation and rupture areas. The researchers are looking for a correlation or ratio between different profile roughness parameters, especially arithmetical mean deviations of the roughness profile Ra and maximum height of the roughness profile Rz, for this case.

1 Introduction

Fracture topography [1] is one of the basic investigations aimed at determining the cause of the damage. It allows determining what kind of the loading the material was subjected. Several typical macroscopic patterns of fatigue damage can be distinguished. Among them there are functions of type and magnitude of loading. The surface analysis reveals localization of initiation and crack path propagation.

Nowadays surface roughness parameters [2] are defined in a handful of international standards [3, 4]. There are more than a hundred parameters describing the surface topography that we divide into three groups, which are defined as amplitude parameters, spacing parameters, and hybrid parameters [5]. The two most popular surface roughness parameters are arithmetical mean deviation of the roughness profile Ra (1) and maximum height of the roughness profile Rz (2). Fig. 1 shows graphically how the Ra and Rz parameters are calculated.

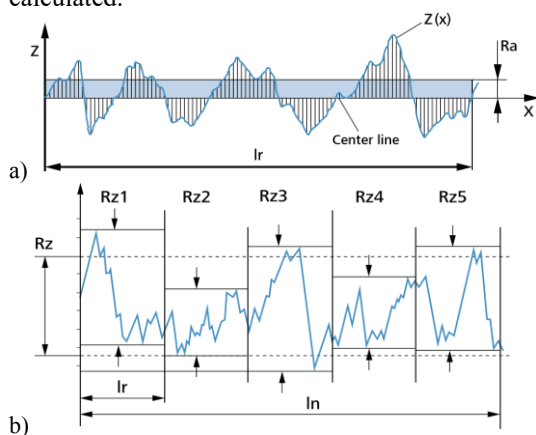


Fig. 1. The surface profiles and the method for calculating parameters a) Ra, b) Rz.

* Corresponding author: w.macek@po.opole.pl

$$Ra = \frac{1}{lr} \int_0^{lr} |Z(x)| dx \quad (1)$$

$$Rz = \frac{Rz1 + Rz2 + Rz3 + Rz4 + Rz5}{5} \quad (2)$$

Ra averages all peaks and valleys of the roughness profile and then neutralizes the few outlying points so that the extreme points have no significant impact on the final results. Rz averages only the five highest peaks and the five deepest valleys, therefore extremes have a much greater influence on the final value.

The results of fracture topography studies, and in particular the roughness profile parameters Ra and Rz, were analysed in this paper.

2 Materials and methods

The following section gives a short description of two kinds of fatigue tests for two materials, both in bending, torsion, and bending with torsion loadings. The method of measuring fracture surface topography is also presented.

2.1 Fatigue tests

2.1.1 Steel S355J2 subjected to non-proportional bending with torsion

Table 1 shows the mechanical properties of the tested steel. Fatigue tests on hourglass specimens, as shown in Fig. 2, with a minimum diameter $d = 8$ mm, made of S355J2 steel, were performed on a MZGS-200PLZ test stand [6, 7]. In order to distinguish the type of loading

stress ratio $r = \tau_{\max} / (\sigma_{\max} + \tau_{\max})$ was employed, amounting from 0 to 0.55. Mean stress effect did not occur and the stress ratio in these studies were $R = 0$.

Table 1. The mechanical properties of the S355J2 steel.

σ_y (MPa)	σ_u (MPa)	E (GPa)	ν (-)
357	535	210	0.30



Fig. 2. The exemplary hourglass specimen after fatigue test.

2.1.2 EN AW-2017A-T4 aluminium alloy subjected to proportional bending with torsion

This material was characterized by the mechanical properties in table 2.

Table 2. The mechanical properties of the EN AW-2017A-T4 aluminium alloy.

σ_y (MPa)	σ_u (MPa)	E (GPa)	ν (-)
382	480	72	0.32

The specimens with rectangular cross-section dimensions 8x10 mm were tested. The specimens had an external, unilateral, sharp and blunt one-sided notches, which radius was $\rho = 0.2$ mm, 5 mm, 10 mm and 22.5 mm. The shape and dimensions of the specimen EN AW-2017A-T4 aluminium alloy for the smallest and largest notch radius, respectively a) $\rho = 0.2$ mm and b) $\rho = 22.5$ mm, are shown in Fig. 3.

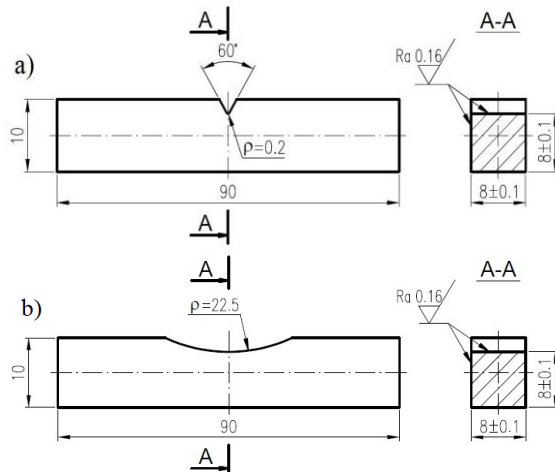


Fig. 3. Shape and dimensions of specimen for: a) $\rho = 0.2$ mm, b) $\rho = 22.5$ mm.

Fatigue tests were performed on a MZGS-100 test stand [8]. In order to distinguish the type of loading stress ratio $r = \tau_{\max} / (\sigma_{\max} + \tau_{\max})$ was employed, amounting from 0 to 1. The stress ratios for this research were $R = -1, -0.5, 0$.

2.2 Fracture study

The study of fracture surfaces was carried out by employing the InfiniteFocus® IF G4 focus variation microscope, produced by Alicona Imaging, shown in Fig. 4. The lateral and vertical travel range (x-y-z axes) of the instrument was 100x100x100 mm³. The measurement device was equipped with a motorized nosepiece using five dedicated microscopic objective lenses from 2.5x to 100x magnification.



Fig. 4. Focus variation microscope InfiniteFocus® IF G4 produced by Alicona Imaging.

The InfiniteFocus® IF G4 focus variation [5, 9] microscope was supported by IF-MeasureSuit 5.1 software produced by Alicona Imaging and by advanced MountainsMap® Universal 7.4 software provided by Digital Surf.

3 Results and discussion

This section includes visualization of the fracture geometry along with an exemplary fracture profiles, and the presentation of roughness Ra and Rz results. The results were used for a brief analysis.

3.1 Fracture geometry

Fig. 5 demonstrates exemplary scanned fractures with marked propagation and rupture area, for 10x magnifications. All exemplified specimens shown in Fig. 4 were made from EN AW-2017A-T4 aluminium alloy and have the same notch radius $\rho = 0.2$ mm.

Fig. 6 shows exemplary 3D views of the surface topography of propagation and rupture area, for the 100x magnifications.

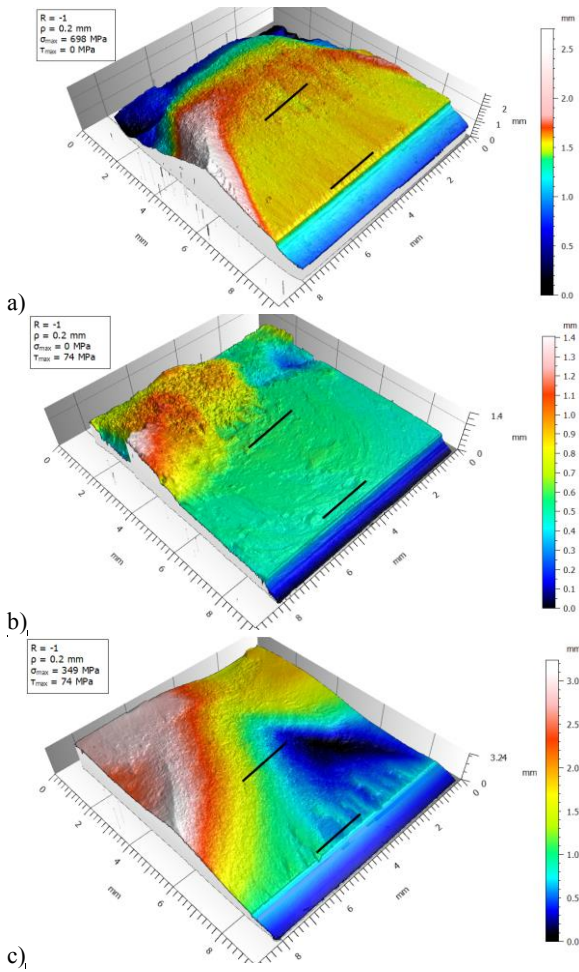


Fig. 5. EN AW-2017A-T4 specimens with marked crack propagation and rupture roughness profiles, for exemplary specimens loadings subjected to a) bending, b) torsion, c) bending with torsion.

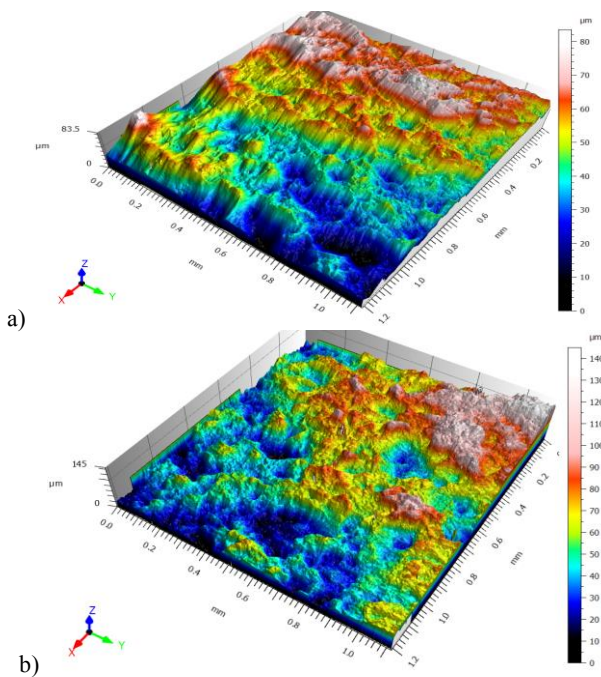


Fig. 6. Roughness surface steel S355J2 specimen subjected to combined bending-torsion loading, with magnitude 100x, for a) the propagation area, b) the rupture area.

Fig. 7 demonstrates exemplary fracture roughness profile a) propagation and b) rupture area, for EN AW-2017A-T4 specimen subjected to bending loading and $r=0$.

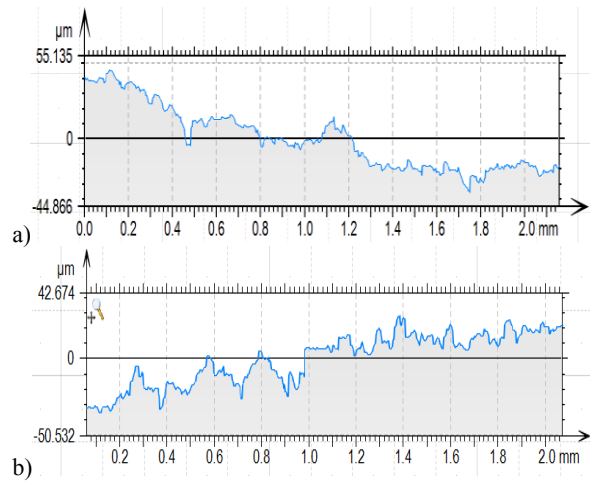


Fig. 7. The profile diagram of EN AW-2017A-T4 specimen subjected to bending loading, $r=0$, for a) the propagation area, b) the rupture area.

3.2 Roughness parameters analysis

Propagation and rupture profiles were measured for representative 2 mm profile length as marked in Fig. 5. For the sake of great impact of filter waviness λc , on roughness measurements [3, 4], constant value $\lambda c = 250 \mu\text{m}$ was used.

Rz and Ra roughness parameters were used for the analysis in the areas of propagation and rupture. The Rz/Ra factor relationship to r parameter was also checked for propagation and rupture area.

Fig. 8 shows the relationship between Rz and Ra of propagation area for both EN AW-2017A-T4 and S355J2 materials.

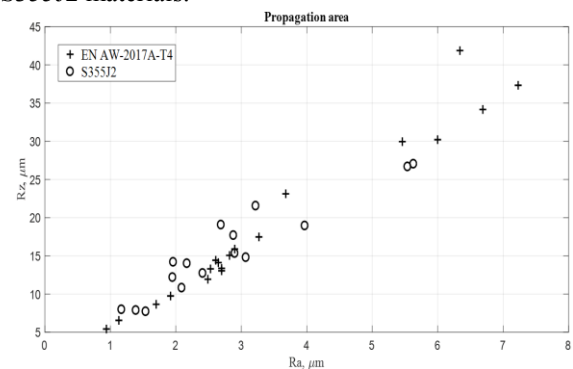


Fig. 8. The relationship between Rz and Ra of propagation area.

The mean value Ra for propagation amounted to $Ra=3.46\mu\text{m}$ for EN AW-2017A-T4, and $Ra=2.79\mu\text{m}$ for S355J2. On the other hand, respectively $Rz=18.71\mu\text{m}$ and $Rz= 15.53\mu\text{m}$.

The dependence of Rz to Ra on the rupture area is shown in Fig. 9.

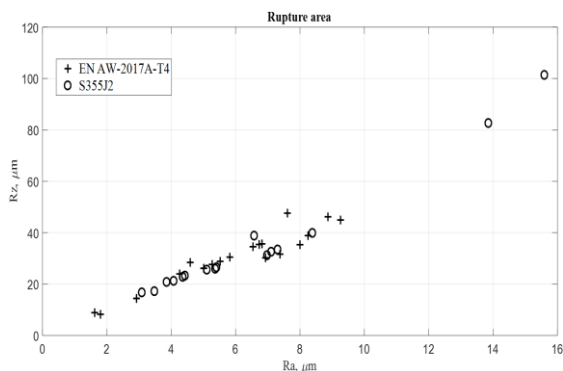


Fig. 9. The relationship between Rz and Ra of rupture area.

For rupture area, the mean value of roughness, is for EN AW-2017A-T4 $Ra=5.96\mu m$, $Rz=30.40\mu m$ and by analogy for S355J2 $Ra=6.56\mu m$, $Rz=34.93\mu m$.

Comparing data from the graphs in Figures 8 and 9, we can infer that regardless of the method of loading and the type of notch, on average for EN AW-2017A-T4 the tested specimens Ra is 1.88 times bigger for rupture than for propagation area. Similarly Rz, for the same material, is 1.80 times bigger. While for S355J2 all tested specimens Ra and Rz are respectively 2.64 and 2.37 times bigger for rupture than for propagation area.

Fig. 10 and Fig. 11 show the relationship of Rz/Ra to r parameter respectively for propagation area and the rupture area, in a comprehensive overview, for all types of fatigue tests being analysed.

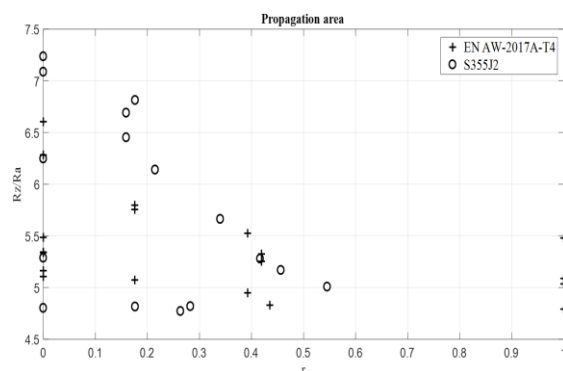


Fig. 10. The Rz/Ra factor relationship to r parameter, for initiation area.

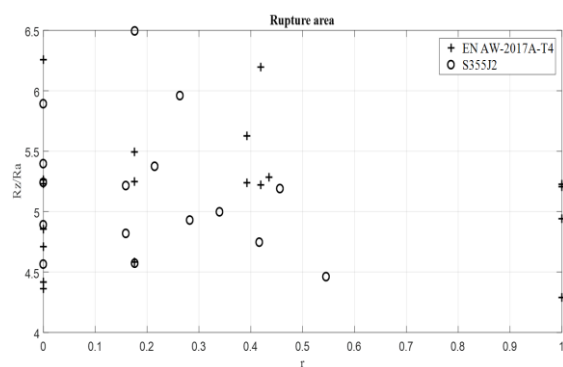


Fig. 11. The Rz/Ra factor relationship to r parameter, for rupture area.

Independent on stress ratio R, notch radius p, loading ratio r and form of fatigue, the following information was extracted:

- for propagation areas of S355J2 specimens, the mean value amounts to $Rz/Ra=5.77$,
- for rupture areas of S355J2 specimens, the mean value is $Rz/Ra=5.17$,
- for propagation areas of EN AW-2017A-T4, the mean value reaches $Rz/Ra=5.38$,
- for rupture areas of EN AW-2017A-T4, the mean value totals $Rz/Ra=5.14$.

The increase in the share of torsional loading components increases the roughness of the fracture surface, however, there was no similar dependence between Rz/Ra and r.

4 Conclusions

Different fatigue tests produce different surface characteristics. On the above experimental results, it can be stated that both roughness parameters Ra and Rz grow along with the increase in the proportion of torsional loadings. For steel tested the differences between the rupture and propagation areas were higher for Ra (1.88) rather than Rz (1.80), when for aluminium alloy, the results were 2.64 and 2.37 respectively. Rz/Ra ratio amounted from 4.29, for AW-2017A-T4 in rupture area to 7.23, for S355J2 in propagation area. Rz averages the highest peaks and the deepest valleys, therefore extremes have a much greater influence on the final value, than Ra parameter.

References

1. K. Slámečka, J. Pokluda, P. Ponížil, S. Major, P. Šandera, Eng. Fract. Mech., **75**(3-4), 760-767(2008)
2. E.S. Gadelmawla, M.M. Koura, T.M. Maksoud, I.M. Elewa, & H.H. Soliman, J. Mater. Process. Tech., **123**(1), 133-145 (2002)
3. ISO 25178-2:2012 - Geometrical product specifications (GPS) — Surface texture: Areal — Part 2: Terms, definitions and surface texture parameters.
4. ASME B46.1-2009, Surface Texture, Surface Roughness, Waviness and Lay.
5. Leach R. (Ed.): Optical Measurement of Surface Topography, Springer-Verlag Berlin Heidelberg (2011)
6. Z. Marciniak, D. Rozumek, E. Macha, Int. J. of Fatigue, **58**, 84-93 (2014)
7. W. Macek, E. Macha, Arch. Mech. Eng., **62**(1) 85-100 (2015)
8. S. Faszynka, D. Rozumek, Solid State Phenomena, **250**, 10-15, 2016,
9. N.I. Nikolaev, J.N. Petzing, J.M. Coupland, Appl. Optics., **55**(13), 3555-3565 (2016)